Original Article

The structural MRI markers and cognitive decline in prodromal Alzheimer's disease: a 2-year longitudinal study

Hongchun Wei[1#], Min Kong[2#], Chunhua Zhang[1], Lina Guan[1], Maowen Ba[1]; for Alzheimer's Disease Neuroimaging Initiative[*]

[1]Department of Neurology, The Affiliated Yantai Yuhuangding Hospital of Qingdao University, Yantai 264000, China; [2]Department of Neurology, Yantaishan Hospital, Yantai 264000, China

[#]These authors contributed equally to this work.

Correspondence to: Maowen Ba. Department of Neurology, The Affiliated Yantai Yuhuangding Hospital of Qingdao University, Yantai 264000, China. Email: bamaowen@163.com.

Background: Being clinically diagnosed with a mild cognitive impairment (MCI) due to Alzheimer's disease (AD) is widely studied. Yet, the clinical and structural neuroimaging characteristics for prodromal AD, which are defined as A+T+MCI based on the AT (N) system are still highly desirable. This study evaluates the differences of the cognitive assessments and structural magnetic resonance imaging (MRI) between the early MCI (EMCI) and late MCI (LMCI) participants based on the AT (N) system. The potential clinical value of the structural MRI as a predictor of cognitive decline during follow-up in prodromal AD is further investigated.

Methods: A total of 406 MCI participants from the Alzheimer's Disease Neuroimaging Initiative (ADNI) database were chosen and dichotomized into EMCI and LMCI groups according to the Second Edition (Logical Memory II) Wechsler Memory Scale. Multiple markers' data was collected, including age, sex, years of education, ApoE4 status, cerebrospinal fluid (CSF) biomarkers, standardized uptake values ratios (SUVR) means of florbetapir-PET-AV45, cognitive measures, and structural MRI. We chose 197 A+T+MCI participants (prodromal AD) with positive biomarkers of Aβ plaques (labeled "A") and fibrillar tau (labeled "T"). We diagnosed Aβ plaques positive by the SUVR means of florbetapir-PET-AV45 (cut-off >1.1) and fibrillar tau positive by CSF phosphorylated-tau at threonine 181 (p-tau) (cut-off >23 pg/mL). The differences of cognitive assessments and regions of interest (ROIs) defined on the MRI template between EMCI and LMCI were compared. Furthermore, the potential clinical utility of the MRI as the predictor of cognitive decline in prodromal AD was evaluated by investigating the relationship between baseline MRI markers and cognition decline at the follow-up period, through a linear regression model.

Results: The LMCI participants had a significantly more amyloid burden and CSF levels of total t-tau than the EMCI participants. The LMCI participants scored a lower result than the EMCI group in the global cognition scales and subscales which included tests for memory, delayed recall memory, executive function, language, attention and visuospatial skills. The cognition levels declined faster in the LMCI participants during the 12- and 24-month follow-up. There were significant differences in ROIs on the structural MRI between the two groups, including a bilateral entorhinal, a bilateral hippocampus, a bilateral amygdala, a bilateral lateral ventricle and cingulate, a corpus callosum, and a left temporal. The thickness average of the left entorhinal, the left middle temporal, the left superior temporal, and the right isthmus cingulate was a

* Data used in preparation of this article was obtained from the Alzheimer's Disease Neuroimaging Initiative (ADNI) database (adni.loni.usc.edu). As such, the investigators within the ADNI contributed to the design and implementation of the ADNI and/or provided data, but they did not participate in analysis or writing of this report. A complete listing of the ADNI investigators can be found at: http://adni.loni.usc.edu/wp-content/uploads/how_to_apply/ADNI_Acknowledgement_List.pdf

main contributor to the decreased global cognition levels. The thickness average of the left superior temporal and bilateral entorhinal played a key role in the memory domain decline. The thickness average of the left middle temporal, and the right isthmus cingulate was significantly associated with an executive function decline.

Conclusions: Based on the AT (N) system, surely, both the EMCI and LMCI diagnoses presented significant differences in multiple cognition domains. Signature ROIs from the structural MRI tests had correlated a cognitive decline, and could act as one potential predictive marker.

Keywords: Alzheimer's disease (AD); structural magnetic resonance imaging (structural MRI); cognitive decline; prodromal AD

Submitted Jul 11, 2018. Accepted for publication Oct 16, 2018.
doi: 10.21037/qims.2018.10.08
View this article at: http://dx.doi.org/10.21037/qims.2018.10.08

Introduction

Alzheimer's disease (AD) is a chronic neurodegenerative disease clinically characterized by the patient's cognitive ability worsening and having an impairment for daily activities. It is pathologically characterized by amyloid-beta (Aβ) plaques levels and presence of neurofibrillary tangles (1,2). Mild cognitive impairment (MCI) is an intermediate stage between cognitively normal status and AD (3).

There is no definitive cure for AD. It is widely believed that the disease progression is slow during the early or preclinical stages (4), and the effective and preventive treatments are needed at early phases of the AD spectrum (5). Thus, there is an increasing amount of attention for the identification of the clinical cognitive decline among MCI individuals.

For a long time, the non-invasive and cost-effective neuropsychological assessments played a crucial role in the identification of the loss of cognitive functions and change in the behavioral and the functional states from normal conditions (6). The fifth edition of the Diagnostic and Statistical Manual of Mental Disorders (DSM-5) (7) has defined six key domains of cognition to look at. Identifying the dysfunction of such domains and sub-domains has helped to establish the etiology and severity of the neurocognitive disorder. Many researchers found that the amnestic MCI (aMCI) patients with a memory domain impairment had an 8.5 greater times of risk to develop AD than those MCI patients without memory dysfunction (8). For many years, AD was conceived as a clinical-pathological construct, it was assumed that if individuals had the typical amnestic multi-domains symptoms, they would have AD neuropathological changes at their autopsy (9). However, the diagnostic accuracy of the above methods was low. By now, it is well established that this theory does not correlate with the AD pathologic change at the time of the autopsy (6,10,11). An individual diagnosed with MCI could be at risk of later developing AD, or it could be due to age-related memory decline or other neurodegenerative diseases. Therefore, the research based on this classification would also deviate.

In 2018, the National Institute on Aging and Alzheimer's Association (NIA-AA) has proposed a research framework, which is labeled the AT (N) system. The scheme recognizes three general groups of biomarkers based on the nature of the pathologic process (12). In accordance with this scheme, we selected the A+T+MCI participants named prodromal AD by the SUVR means of florbetapir-PET-AV45 (cut-off >1.1) (13) and the cerebrospinal fluid (CSF) p-tau levels (cut-off >23 pg/mL) (14). We expected to study the characteristics of the clinical cognition levels and structural magnetic resonance imaging (MRI) tests in the MCI patients, who had a more pathologically consistent diagnosis with the changes of AD. The relationship between the structural MRI tests and a cognitive decline was also evaluated in prodromal AD. We hypothesized that some baseline signature ROIs of the structural MRI scan would be related with cognitive function decline, and that the smaller volume or thickness of a specific region would be associated with cognitive decline. Finally, we also hypothesized that the atrophy of a specific region would potentially correlate with different patterns of cognition

decline throughout the pathophysiological process of AD.

Methods

ADNI and subjects

Data used in the preparation of this article was obtained from the Alzheimer's Disease Neuroimaging Initiative (ADNI) database (http://adni.loni.usc.edu). Specifically, we downloaded the following information in August 2016, including age, sex, years of education, ApoE4 status (participants were divided into ApoE4 (+/+), ApoE4 (+/–) and ApoE4 (–/–) carriers according to having two or one or no copies of the allele 4), CSF biomarkers, SUVR means of florbetapir-PET-AV45, structural MRI, and cognitive measures at the baselines 12- and 24-month follow-up. For more up-to-date information, see http://www.adni-info.org.

In this study, we selected 406 subjects with MCI from the ADNI2 and ADNI-GO groups who had a subjective memory complaint, objective memory loss measured by using education-adjusted scores on the Logical Memory II (Delayed Recall) subscale of the Wechsler Memory Scale, a CDR of 0.5, preserved activities of daily living, and an absence of dementia. We excluded MCI due to non-AD, such as unknown or uncertain etiology, aging, small vessel disease, stress, depression, medication and demyelination disease, and subjects without complete information. In total, we chose 197 A+T+MCI participants, who had positive biomarkers of Aβ plaques and fibrillar tau as described above. The participants were further diagnosed as 100 EMCI and 97 LMCI participants by the ADNI-2 procedures manual criteria (http://www.adni-info.org). The EMCI group differed from the LMCI one, only based on the education-adjusted scores for the delayed paragraph recall sub-score on the Wechsler Memory Scale–Revised Logical Memory II.

Standard protocol approvals, registrations, and patient consents

The ADNI was approved by the institutional review board at each site and was compliant with the Health Insurance Portability and Accountability Act. Written consent could be obtained from all participants at each site.

Florbetapir-PET-AV45

We also obtained the SUVR means of florbetapir-PET-AV45 (average presumes, prefrontal, orbitofrontal, parietal, temporal, anterior, and posterior cingulate cortices) to calculate the amyloid burden. Further details regarding ADNI image acquisition and processing can be found at www.adni-info.org/methods. The data from the cortical amyloid burden via SUVR on florbetapir-PET-AV45 was obtained from the ADNI files 'UCBERKELEYAV45_06_15 _16.csv'. The neuroimaging techniques used by ADNI have been reported previously (15). We diagnosed the amyloid as being positive according to the SUVR cut-off value of 1.1 (13).

CSF data

CSF Aβ1-42, total tau (t-tau) and p-tau were measured by using Innogenetics (INNO-BIA AlzBio3) immunoassay kit-based reagents in the multiplex xMAPLuminex platform (Luminex) as previously described (14). The CSF data used in this study was obtained from the ADNI files 'UPENNBIOMK5-8.csv'. Detailed ADNI methods for CSF acquisition, measurements and quality control procedures were described at www.adni-info.org. In order to select subjects with fibrillar tau (T+), we applied p-tau autopsy-validated positivity cutoffs of 23 pg/mL to determine positivity as described previously (14).

Neuropsychological assessment

All MCI subjects underwent 31 neuropsychological assessments, starting from their baseline visit to the 12 and 24 months follow-up visits. We utilized Clinical Dementia Rating Sum of Boxes (CDR-SB), Alzheimer's Disease Assessment Scale-Cognitive subscale (ADAS-Cog) consisting of 11 (ADAS-Cog 11) and 13 items (ADAS-Cog 13), Mini-Mental State Examination (MMSE), Montreal Cognitive Assessment (MoCA), Functional Assessment Questionnaire (FAQ) to assess the global cognition, the Rey Auditory Verbal Learning Test (RAVLT) and ADNI-MEM to evaluate memory function, the ADNI-EF to evaluate executive function, the Boston Naming Test (BNT) and Category Fluency Tests to evaluate language function. In addition to the above psychometric measures, we also examined the measurement of cognitive complaints via the Everyday Cognition (ECog) questionnaire, using both informant-reports and self-reported data.

The value of cognitive decline is defined as the cognitive scale at 12- and 24-month follow-up time, minus the baseline scale.

MRI imaging

These scans on 197 subjects were performed on the 1.5 T MRI scanners by using a sagittal MPRAGE sequence with the following parameters: repetition time (TR) =2,400 ms, inversion time (TI) =1,000 ms, flip angle =8°, and field of view (FOV) =24 cm with a 256×256×170 acquisition matrix in the x-, y-, and z-dimensions, which yields a voxel size of 1.25×1.261×2. All of the original source and unmodified image files are available to the general scientific community, as described at http://www.loni.ucla.edu/ADNI.

The MRI data that was preprocessed by using the standard procedures included a realignment of the anterior commissure and posterior commissure, using the MIPAV software, skull-stripping by using Brain Surface Extractor (BSE) and Brain Extraction Tool (BET). The cerebellum removal, intensity inhomogeneity correction, segmentation was done using the FSL-FAST software, and spatial co-registration by using HAMMER (16,17). T1 MRI images from the ADNI database were automatically partitioned into many regions of interest (ROIs) spanning the entire brain with the FreeSurfer image analysis suite. The instructions located on the FreeSurfer methods citation webpage: http://surfer.nmr.mgh.harvard.edu/fswiki/FreeSurferMethodsCitation. In the validation experiments, this FreeSurfer processing approach achieved significantly high accuracy. The ADNI staff members have finished MRI Image processing work. One hundred and seven ROIs were automatically segmented according to the label on the Jacob atlas, defined by FreeSurfer (18), and then the EMCI and LMCI groups were compared. At last, 34 ROIs were selected in combination with the existing literature results (19), which may significantly influence MCI progression. The 34 ROIs included the surface area of bilateral posterior cingulate, thickness standard deviation of the bilateral rostral anterior cingulate, surface area of the right paracentral, thickness average of the left middle temporal and left superior temporal, thickness average and cortical volume of the bilateral isthmus cingulate, the thickness average and cortical volume of the bilateral entorhinal cortices, bilateral hippocampal formation, and bilateral amygdala. Also, the cortical volume of left middle temporal, left superior temporal, left paracentral, right thalamus, and right parahippocampal were included. Subcortical volume of the bilateral lateral ventricle, bilateral inferior lateral ventricle, and the bilateral choroid plexus were selected to reflect the condition of ventricle. Corpus callosum central, mid-posterior, mid-anterior, anterior were selected to reflect the condition of the corpus callosum. The structural MRI neuroimaging data was obtained from the ADNI file 'UCSFFSL_11_02_15', and 'UCSFFSX51_11_02_15_V2'.

Statistical methods

Statistical analysis was performed by using the SAS, version 9.4 software (SAS Institute Inc.). Demographic data (age, gender, educational level, and ApoE4 status), cognitive scores, MRI volumes and thicknesses of ROIs, SUVR means of florbetapir-PET-AV45 and CSF biomarker values were summarized. Between the EMCI and LMCI groups, gender and ApoE4 status were compared using the Chi-square tests for the categorical variables; while age, educational level, SUVR means of florbetapir-PET-AV45 and CSF biomarker values were compared using the independent samples of the t-test for the continuous variables. If each group does not satisfy the normality or homogeneity of variance, we adopted the Wilcoxon rank sum tests. We compared the differences in the cognitive scores of the baseline, 1- and 2-year follow-up, as well as the baseline MRI volumes and thicknesses of ROIs between the two groups by a multivariate analysis of the variance, adjusted by age, gender, years of education, ApoE4 status, and cognitive scores at the baseline when appropriate. Finally, ROIs of the baseline structural MRI, and cognitive decline in 1- and 2-year follow-up were assessed with a linear regression model. Age, gender, years of education, ApoE4 status, and cognitive scores at the baseline were included in models. $P<0.05$ was adopted and regarded to the significance.

Results

Baseline characteristics of EMCI participants in comparison with LMCI

Baseline demographics, ApoE4 status, and biomarker characteristics of the two groups are summarized in the *Table 1*. Overall, EMCI and LMCI participants had no difference in age, CSF Aβ1-42 and p-tau, sex composition and proportion of ApoE4 status. But the LMCI group had significantly more t-tau levels and an amyloid burden than the EMCI group (P=0.011, 0.016). Both groups had a statistically significant difference in the years of

Table 1 Baseline demographics and sample characteristics in EMCI and LMCI

Demographics	EMCI	LMCI	P value
No. of subjects	100	97	
Age, years	73.09±6.701	72.54±6.880	0.886
Male, n (%)	60 (60.00)	50 (51.55)	0.232
Education, years	15.70±2.844	16.58±2.657	0.034*
ApoE4, n (%)			0.219
ApoE4 (–/–)	35 (35.00)	23 (23.71)	
ApoE4 (+/–)	49 (49.00)	55 (56.70)	
ApoE4 (+/+)	16 (16.00)	19 (19.59)	
Aβ1-42	140.05±30.399	134.51±23.374	0.272
T-tau	108.43±55.988	124.34±52.685	0.011*
P-tau$_{181P}$	53.92±21.443	59.32±27.105	0.193
Florbetapir-PET global SUVR	1.37±0.152	1.42±0.173	0.016*

*, statistically significant. EMCI, early mild cognitive impairment; LMCI, late mild cognitive impairment; APOE, apolipoprotein E; Aβ, β-amyloid; P-tau$_{181P}$, tau phosphorylated at threonine 181; florbetapir-PET global SUVR, uptake values ratios (SUVR) means of florbetapir-PET-AV45.

education (P=0.034).

Neuropsychological examinations

As expected, the EMCI and LMCI groups showed significant differences in neuropsychological assessments at the baseline and at the 12-, 24-month-visit as highlighted in *Table 2*. LMCI participants performed worse in the domains of global cognition scales and subscales including memory, delayed recall memory, executive, language, attention and visuospatial skills compared to those of LMCI. To be specific, the LMCI participants had higher mean CDR-SB score (1.95±0.924 versus 1.46±0.895, P<0.001), higher mean ADAS13 score (21.02±7.136 versus 14.43±5.252, P<0.001), higher mean FAQ score (4.64±4.400 versus 2.91±3.962, P<0.001), lower mean MMSE score (27.09±1.882 versus 27.99±1.761, P<0.001), lower mean MoCA score (21.78±2.884 versus 23.40±2.966, P<0.001) at the baseline. In the subscale of memory, participants of LMCI had worse performance than those of EMCI manifested by RAVLT (RAVLT-immediate, learning, forgetting and perc-forgetting) and ADNI-MEM. In the executive function assessment (ADNI-EF), LMCI participants had a worse performance than the EMCI group (–0.02±0.800 versus 0.38±0.826, P<0.001). These findings were also consistent with the Category Fluency Tests (Animals and Vegetables), Clock test, Boston Naming Test, Trail Making Test A and B, which respectively assessed for executive function, language, attentiveness, and visuospatial skills. Participants with LMCI had a higher informant-report ECog scores (Everyday Memory, Language, Visuospatial Abilities, Planning, Organization, and Divided Attention) than the EMCI participants. However, the two groups showed no difference in the self-report ECog scores. Furthermore, we followed these patients at the 12- and 24-month and arrived at the same conclusions.

Similarly, LMCI subjects demonstrated a worse cognitive performance than the EMCI subjects on their decline of neuropsychological examinations during the 12 months' change from baseline, and the differences were even greater in the 24 months' change (*Figure 1*).

ROIs in structural MRI

We investigated the differences of 107 ROIs obtained from the structural MRI between EMCI and LMCI, 30 of them had significant differences. We found that the individuals in LMCI group had substantially smaller volume of the bilateral hippocampus, right parahippocampal, left middle and superior temporal, bilateral amygdala, bilateral cingulate, both thickness average, and cortical volume of bilateral entorhinal (*Figure 2*). The LMCI group had

Table 2 Cognitive assessments comparison between EMCI and LMCI at baseline, 12-month, 24-momth visit

Cognitive assessments	Baseline			12 months			24 months		
	EMCI (N=100)	LMCI (N=97)	Adjusted P	EMCI (N=100)	LMCI (N=97)	Adjusted P	EMCI (N=100)	LMCI (N=97)	Adjusted P
CDR-SB	1.46±0.895	1.95±0.924	<0.001**	1.73±1.447	2.65±1.279	<0.001**	2.02±1.654	4.03±2.551	<0.001**
ADAS11	8.73±3.159	12.95±5.249	<0.001**	8.96±3.914	14.12±6.157	<0.001**	9.14±4.113	17.51±7.610	<0.001**
ADAS13	14.43±5.252	21.02±7.136	<0.001**	14.51±5.874	22.45±8.293	<0.001**	14.62±6.434	26.46±10.153	<0.001**
MMSE	27.99±1.761	27.09±1.882	<0.001**	27.62±1.773	25.72±2.572	<0.001**	27.46±2.009	24.44±3.346	<0.001**
FAQ	2.91±3.962	4.64±4.400	0.003*	3.93±4.814	7.30±6.070	<0.001**	4.24±5.511	10.54±8.252	<0.001**
MOCA	23.40±2.966	21.78±2.884	<0.001**	23.23±2.776	21.45±3.335	<0.001**	23.15±3.206	19.97±4.246	<0.001**
RAVLT-immediate	35.71±9.551	30.22±8.932	<0.001**	34.80±10.360	27.93±9.516	<0.001**	35.73±9.800	26.18±10.755	<0.001**
RAVLT-learning	4.68±2.482	3.25±2.296	<0.001**	4.14±2.288	2.71±2.429	<0.001**	4.45±2.622	2.01±1.997	<0.001**
RAVLT-forgetting	4.91±2.310	5.48±2.292	0.229	5.33±2.678	5.30±2.271	0.906	5.54±2.847	5.00±2.239	0.065
RAVLT-perc-forgetting	58.00±28.673	78.05±26.906	<0.001**	66.89±31.318	84.74±25.484	<0.001**	65.12±31.905	88.14±24.526	<0.001**
EcogPtMemory	2.33±0.654	2.45±0.669	0.229	2.42±0.715	2.35±0.736	0.41	2.43±0.705	2.34±0.829	0.501
EcogPtLanguage	1.89±0.644	1.84±0.673	0.868	1.93±0.651	1.80±0.752	0.367	1.90±0.545	1.79±0.778	0.42
EcogPtVisuospatial abilities	1.50±0.590	1.48±0.578	0.681	1.50±0.546	1.52±0.630	0.828	1.50±0.572	1.54±0.631	0.736
EcogPtPlanning	1.54±0.612	1.49±0.580	0.743	1.57±0.618	1.48±0.580	0.422	1.51±0.550	1.46±0.575	0.827
EcogPtOrganization	1.63±0.650	1.58±0.581	0.731	1.68±0.686	1.61±0.623	0.675	1.65±0.684	1.56±0.603	0.488
EcogPtDivided attention	1.99±0.792	1.85±0.675	0.126	2.05±0.816	1.93±0.793	0.294	1.94±0.707	1.83±0.676	0.388
EcogPtTotal	1.84±0.539	1.82±0.521	0.851	1.88±0.568	1.81±0.601	0.467	1.85±0.498	1.80±0.600	0.612
EcogSPMemory	2.26±0.811	2.68±0.770	0.001*	2.31±0.852	2.86±0.826	<0.001**	2.45±0.887	3.11±0.862	<0.001**
EcogSPLanguage	1.75±0.719	1.96±0.767	0.032*	1.80±0.742	2.12±0.808	0.006*	1.92±0.873	2.43±0.948	<0.001**
EcogSPVisuospatial abilities	1.47±0.648	1.71±0.714	0.036*	1.49±0.717	1.93±0.797	0.001*	1.67±0.811	2.30±0.985	<0.001**
EcogSPPlanning	1.58±0.704	1.86±0.783	0.012*	1.70±0.792	2.07±0.897	0.007*	1.81±0.867	2.42±1.031	<0.001**
EcogSPOrganization	1.65±0.751	1.94±0.864	0.028*	1.82±0.863	2.18±1.026	0.041*	1.85±0.833	2.58±1.084	<0.001**
EcogSPDivided attention	2.00±0.908	2.15±0.869	0.275	2.16±0.948	2.46±0.950	0.069*	2.19±0.970	2.84±0.930	<0.001**
EcogSPTotal	1.80±0.660	2.07±0.661	0.008*	1.88±0.706	2.29±0.758	0.001*	1.99±0.776	2.62±0.862	<0.001**

Table 2 *(continued)*

Table 2 *(continued)*

Cognitive assessments	Baseline			12 months			24 months		
	EMCI (N=100)	LMCI (N=97)	Adjusted P	EMCI (N=100)	LMCI (N=97)	Adjusted P	EMCI (N=100)	LMCI (N=97)	Adjusted P
ADNI-MEM	0.34±0.522	−0.25±0.580	<0.001**	0.27±0.657	−0.43±0.775	<0.001**	0.31±0.665	−0.63±0.854	<0.001**
ADNI-EF	0.38±0.826	−0.02±0.800	<0.001**	0.32±0.822	−0.15±0.910	<0.001**	0.32±0.912	−0.23±1.013	<0.001**
Category Fluency Tests (Animals and Vegetables)	18.39±5.603	16.30±5.044	0.001*	17.39±5.149	14.88±4.921	<0.001**	17.17±5.667	14.03±5.452	<0.001**
Clock test	4.55±0.757	4.16±1.017	<0.001**	4.51±0.692	3.98±1.151	<0.001**	4.50±0.814	4.14±1.174	0.03*
BNT	26.65±3.239	25.08±4.089	0.001*	26.91±3.371	25.15±4.899	0.001*	26.74±3.844	24.36±5.082	0.001*
TMT-A	38.90±17.027	44.27±20.569	0.032*	39.41±18.153	48.00±23.093	0.006*	39.19±14.506	49.49±28.542	0.005*
TMT-B	105.53±56.864	132.20±74.946	0.003**	113.42±65.832	144.10±80.280	0.005*	114.49±69.167	160.28±91.111	0.001*

P values were adjusted by age, gender, years of education, ApoE4 status, and cognitive scores at baseline when appropriate. *, P<0.05; **, P<0.001. CDR-SB, Clinical Dementia Rating Scale-Sum of Boxes; ADAS-Cog11 or 13, Alzheimer's Disease Assessment Scale-11 or 13-Item Subscale; MMSE, Mini-Mental State Examination; FAQ, Functional Assessment Questionnaire; MoCA, Montreal Cognitive Assessment; RAVLT, Rey Auditory Verbal Learning Test; ECog, Test of Everyday Cognition; PT, participant; SP, study-partner; BNT, Boston Naming Test; TMT-A,B, Trail Making Test A,B.

a larger volume of the lateral ventricle. Details of these findings are displayed in *Table 3*.

Associations between ROIs in structural MRI and cognitive decline

Based on the above results, we further selected the signature ROIs and cognitive assessments to study the correlation between the baseline structural MRI and the cognitive decline at the 24-month visit mark from baseline. After adjusting for age, gender, years of education, ApoE4 status, the independent effects of baseline ROIs in the structural MRI on cognitive decline, the subjects were evaluated. The associations between the baseline Imaging biomarkers and cognitive decline at 24 months for all investigated subjects were presented in *Table 4*.

The results indicated that the subcortical volume of the bilateral amygdala, bilateral hippocampus, cortical volume and thickness average of bilateral entorhinal, thickness average of left middle and left superior temporal, cortical volume of left middle temporal were highly correlated with a global cognitive decline, when it was evaluated using CDRSB, ADAS13, MMSE, MoCA, and FAQ. Especially, the thickness average of left entorhinal, left middle temporal, left superior temporal right isthmus cingulate which mainly contributed to the decreased global cognition.

In memory assessment (RAVLT-immediate, ADNI-MEM), we found that cortical volume of left middle temporal, thickness average of left middle temporal, cortical volume of left superior temporal, thickness average of left superior temporal, subcortical volume of bilateral amygdala, subcortical volume of bilateral hippocampus, cortical volume of bilateral entorhinal, thickness average of bilateral entorhinal are more associated with the cognitive decline. Above all, thickness average of the left superior temporal and bilateral entorhinal had the most significant effect on memory decline.

Additionally, cortical volume of left middle temporal, right entorhinal, bilateral amygdala, thickness average of left middle temporal, right isthmus cingulate, surface area of left posterior cingulate, were correlated with decline in the ANDI-EF group. Thickness average of the left middle temporal and the right isthmus cingulate had the most significant impact on the ANDI-EF decline.

Moreover, we also evaluated ROIs' influences on the changes of EcogSPVisspat, EcogSPPlan and EcogSPTotal. The results were shown in *Table 4*.

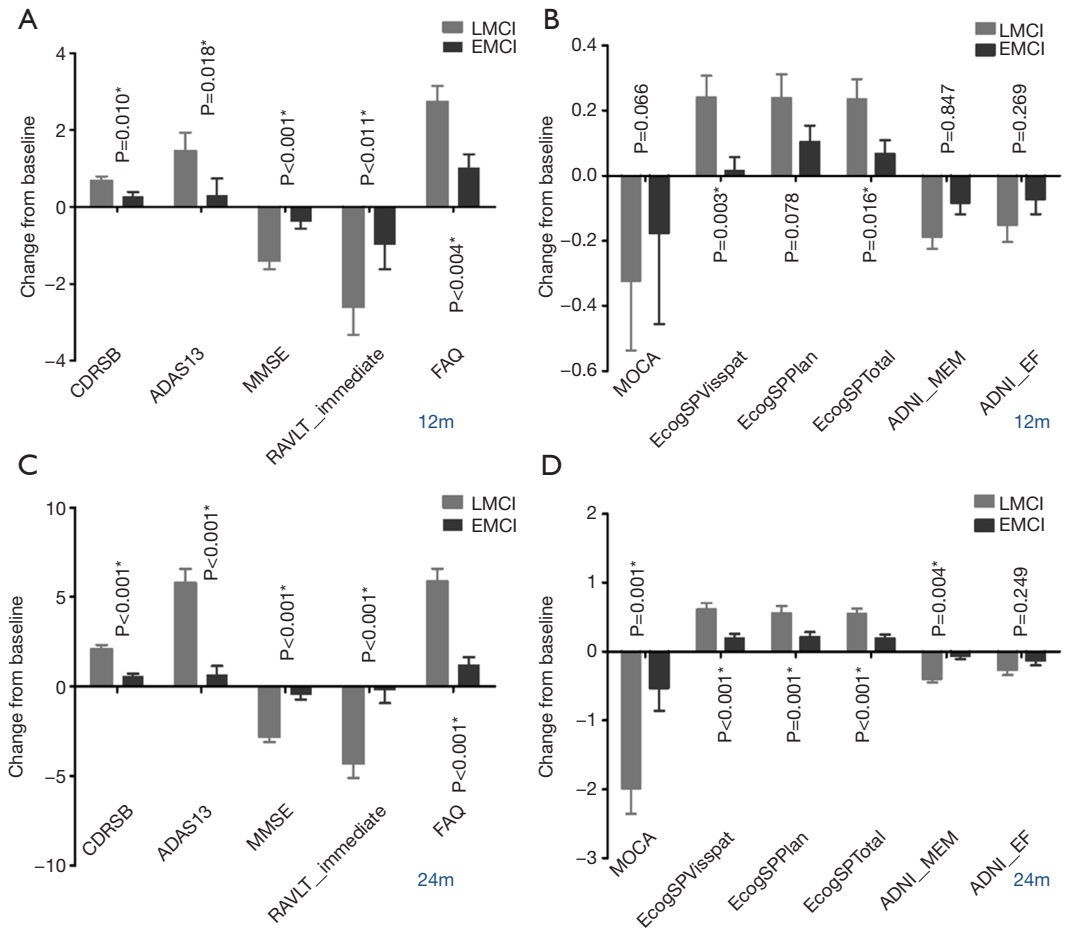

Figure 1 Comparison between EMCI and LMCI in cognitive decline at 12- and 24-month visit. (A,B) Comparison of CDR-SB, ADAS-13, MMSE, RAVLT-immediate, FAQ and MoCA, ECogSPVisspat, ECogSPPlan, ECogSPTotal, ADNI-MEM, ADNI-EF at 12-month visit. (C,D) Comparison of CDR-SB, ADAS-13, MMSE, RAVLT-immediate, FAQ and MoCA, ECogSPVisspat, ECogSPPlan, ECogSPTotal, ADNI-MEM, ADNI-EF at 24-month visit. EMCI, early mild cognitive impairment; LMCI, late mild cognitive impairment; CDR-SB, Clinical Dementia Rating scale Sum of Boxes; ADAS 13, Alzheimer's Disease Assessment Scale-Cognitive subscale consisting of 13 items; MMSE, Mini-Mental State Examination; RAVLT, Rey Auditory Verbal Learning Test; FAQ, Functional Assessment Questionnaire; MoCA, Montreal Cognitive Assessment; ECog, Everyday Cognition questionnaire.

Discussion

This study provided a comprehensive evaluation of the clinical cognitive performance and structural MRI scan of the brain between EMCI and LMCI individuals, who had positive biomarkers of the Aβ plaques and fibrillar tau, based on the AT (N) system. In the present study of prodromal AD, we had three major findings: (I) for the most part, the LMCI group performed significantly worse than the EMCI group in the cognitive tests, including global cognition scales and subscales (memory, executive function, language, attention, visuospatial skills). The LMCI participants had a higher informant-report ECog scores than the EMCI participants. However, the two groups showed no difference in the self-reported ECog scores. (II) For the structural MRI, both groups differed in bilateral entorhinal, hippocampus, amygdala, lateral ventricle, and left temporal, corpus callosum and cingulate. (III) Thickness average of the left entorhinal, left middle and superior temporal, right isthmus cingulate were closely associated with global a cognitive decline. Thickness averages the of left superior temporal and the bilateral entorhinal were more predictive to a memory decline, while the thickness average of left

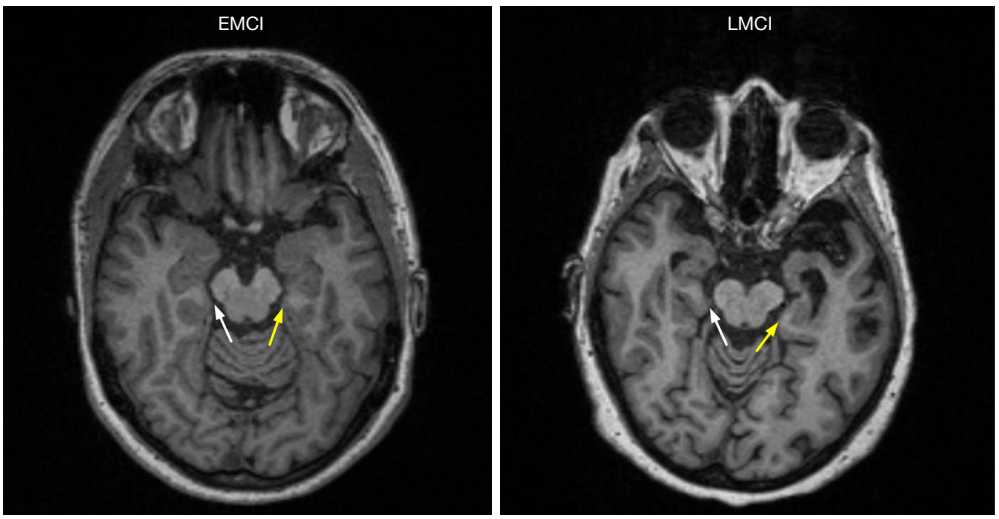

Figure 2 Typical structural head MRI from EMCI and LMCI individuals displaying thickness of bilateral entorhinal. LMCI individual had smaller thickness of bilateral entorhinal. White arrow indicates right entorhinal. Yellow arrow indicates left entorhinal. EMCI, early mild cognitive impairment; LMCI, late mild cognitive impairment.

middle temporal and right isthmus cingulate were associated with executive dysfunction.

As we all know, plaques and tangles define AD as a unique disease among several that can lead to dementia. It is fortunate that biomarkers from the important categories of AD neuropathological change (Aβdeposition, pathologic tau, and neurodegeneration) have been and are being explored. In the 2018 NIA-AA Research Framework, it has stated that both Aβand paired helical filament (PHF) tau deposits are required to fulfill the neuropathological criteria for AD (20,21), which suggests that the evidence of the abnormalities in both the Aβ and the pathologic tau biomarkers should be present to apply the label "Alzheimer's disease" in a living person.

Previous studies have defined probable AD as a prototypical multi-domain amnestic dementia phenotype, and also diagnosed MCI mostly based on the clinical classification, which ignored the AD pathologic changes at autopsy (10,22). Nelson *et al.* had declared that almost 10% to 30% of individuals clinically diagnosed as AD dementia did not display AD neuropathological changes at autopsy. Many studies show that an amnestic multi-domain dementia is neither sensitive nor specific for AD neuropathological change, and cognitive symptoms are not an ideal way to define AD (23,24). There is great value to use structural an MRI test in the assessment of Alzheimer's disease. However, to date, the predictive value of structural MRI tends to range between 80% and 90% in accuracy and there is a possibility that a clinical misdiagnosis relative to the gold standard pathologic diagnosis and/or additional brain pathologies are confounding factors contributing to the reduced structural MRI classification accuracy.

Based on above considerations, we conducted the present study in A+T+MCI participants who were assigned the label "Alzheimer's pathologic change". Although many previous studies have detected the differences even through AD spectrum, yet, the diagnostic criteria is based on clinical cognitive measurements, and the diagnosis credibility remains controversial. Thus, the present study would be more consistent with the AD pathological changes, and the conclusion in clinical characteristics of the MCI individuals would be more accurate.

According to the NIA-AA Research Framework, the A and T levels indicate specific neuropathological changes that define AD, whereas Neurodegenerative/neuronal injury biomarkers (N) and cognitive symptoms are used to stage severity (25). In this study, we found LMCI group had significantly more t-tau (biomarker of neuronal injury) than EMCI group, which further verified the above conclusion. Meanwhile, it also verified that the severity of the disease evaluated by the clinical cognition status was consistent with the results that were evaluated by the N biomarkers. More studies are needed to evaluate the association between them in the future.

In this study, the LMCI group performed significantly worse than the EMCI group in mostly the cognitive

Table 3 Comparison of ROIs from structural MRI between EMCI and LMCI

Regions	EMCI (N=100)	LMCI (N=97)	P value	Adjusted P
Surface area of left posterior cingulate	1115.84±167.417	1065.73±155.122	0.031	0.042*
Surface area of right posterior cingulate	1124.30±185.566	1068.41±163.099	0.027	0.031*
Thickness standard deviation of right rostral anterior cingulate	0.77±0.132	0.80±0.140	0.176	0.052
Thickness standard deviation of left rostral anterior cingulate	0.80±0.136	0.85±0.165	0.041	0.009*
Surface area of right paracentral	1483.69±215.337	1412.42±170.166	0.011	0.011*
Thickness average of left middle temporal	2.72±0.160	2.63±0.223	<0.001	<0.001**
Thickness average of left superior temporal	2.57±0.189	2.50±0.221	0.026	0.004*
Thickness average of left isthmus cingulate	2.43±0.223	2.36±0.201	0.03	0.008*
Thickness average of right isthmus cingulate	2.41±0.223	2.35±0.235	0.055	0.031*
Cortical volume of right isthmus cingulate	2330.60±406.454	2286.34±358.964	0.421	0.531
Cortical volume of left isthmus cingulate	2549.77±465.940	2427.62±368.876	0.044	0.046*
Thickness average of left entorhinal	3.36±0.418	3.01±0.493	<0.001	<0.001**
Thickness average of right entorhinal	3.47±0.453	3.13±0.543	<0.001	<0.001**
Cortical volume of right entorhinal	1767.69±369.528	1553.84±415.618	<0.001	<0.001**
Cortical volume of left entorhinal	1919.85±380.774	1679.43±418.904	<0.001	<0.001**
Subcortical volume of left hippocampus	3516.36±513.152	3155.94±550.111	<0.001	<0.001**
Subcortical volume of right hippocampus	3603.88±528.382	3227.41±546.070	<0.001	<0.001**
Subcortical volume of right amygdala	1423.48±250.484	1303.33±249.324	<0.001	0.001*
Subcortical volume of left amygdala	1358.91±240.002	1227.20±249.513	<0.001	<0.001**
Cortical volume of left middle temporal	9610.36±1384.704	8993.57±1506.254	0.003	0.003*
Cortical volume of left superior temporal	10648.56±1338.043	10172.02±1357.833	0.014	0.011*
Cortical volume of left paracentral	3176.10±545.286	3135.73±491.148	0.588	0.637
Subcortical volume of right thalamus	6222.86±677.001	6028.60±592.605	0.034	0.030*
Cortical volume of right parahippocampal	1975.29±337.148	1871.05±308.147	0.025	0.018*
Subcortical volume of right lateral ventricle	15947.79±8734.742	19187.65±9950.217	0.017	0.001*
Subcortical volume of left lateral ventricle	17525.74±9651.090	21536.20±11570.59	0.009	<0.001**
Subcortical volume of left inferior lateral ventricle	817.94±565.490	1224.66±838.528	<0.001	<0.001**
Subcortical volume of right inferior lateral ventricle	697.84±497.717	1022.76±678.034	<0.001	<0.001**
Subcortical volume of corpus callosum central	373.84±73.657	345.22±66.687	0.005	0.001*
Subcortical volume of corpus callosum mid-posterior	348.64±77.720	315.18±76.580	0.003	0.001*
Subcortical volume of corpus callosum mid-anterior	380.57±89.367	346.49±71.322	0.004	0.001*
Subcortical volume of corpus callosum anterior	787.54±162.406	747.80±145.419	0.074	0.041*
Subcortical volume of right choroid plexus	2278.62±537.081	2387.30±553.381	0.166	0.017*
Subcortical volume of left choroid plexus	1919.21±393.881	1924.63±394.931	0.924	0.380

*, P<0.05; **, P<0.001.

Table 4 Associations between ROIs in structural MRI and cognitive decline at 24-month

Regions	Coefficience/ P value	CDRSB	ADAS 13	FAQ	MOCA	MMSE	ADNI-MEM	RAVLT-immediate	RAVLT-perc-forgetting	EcogSPVisspat	EcogSPPlan	EcogSTotal	ADNI-EF
Subcortical volume of right inferior lateral ventricle	β	0.001	0.003	0.002	−0.001	−0.002	0	−0.001	0.008	0	0	0	0
	P	0.001*	0.023*	0.013*	0.164	<0.001**	0.408	0.212	0.055	0.001*	0.003*	<0.001**	0.307
Cortical volume of left isthmus cingulate	β	−0.001	−0.003	−0.003	0.001	0	0	0.002	−0.005	0	0	0	0
	P	0.009*	0.024*	0.008*	0.485	0.611	0.019*	0.319	0.417	0.035*	0.153	0.119	0.412
Subcortical volume of corpus callosum central	β	−0.004	−0.013	−0.02	0	0.004	0.001	0.002	0.008	−0.003	−0.004	−0.003	0.001
	P	0.076	0.08	0.003*	0.926	0.22	0.174	0.816	0.82	0.003*	<0.001**	<0.001**	0.452
Cortical volume of left middle temporal	β	0	−0.002	−0.001	0.001	0.001	0	0.002	−0.001	0	0	0	0
	P	0.002*	<0.001**	<0.001**	0.003*	0.003*	<0.001**	<0.001**	0.697	<0.001**	0.009*	<0.001**	0.003*
Thickness average of left middle temporal	β	−2.437	−9.875	−9.994	5.283	5.183	0.787	10.29	−10.938	−1.127	−0.977	−0.832	0.621
	P	0.001*	<0.001**	<0.001**	<0.001**	<0.001**	<0.001**	<0.001**	0.355	<0.001**	0.003*	<0.001**	0.02*
Surface area of left posterior cingulate	β	−0.002	−0.008	−0.009	0.001	0.001	0.001	0.005	−0.013	−0.001	−0.001	−0.001	0.001
	P	0.013*	0.013*	0.003*	0.38	0.639	0.01*	0.214	0.381	0.007*	0.084	0.026*	0.013*
Thickness standard deviation of left rostral anterior cingulate	β	2.824	1.097	6.592	−1.847	−2.981	−0.2	−0.997	28.055	0.781	1.208	0.771	−0.011
	P	0.009*	0.764	0.036*	0.315	0.064	0.431	0.809	0.082	0.062	0.007*	0.024*	0.976
Cortical volume of left superior temporal	β	0	−0.001	−0.001	0	0	0	0.001	0.002	0	0	0	0
	P	0.06	0.054	0.003*	0.405	0.416	0.006*	0.005*	0.363	0.01*	0.104	0.038*	0.3
Thickness average of left superior temporal	β	−2.687	−6.139	−8.349	3.615	3.796	0.764	12.287	−9.525	−0.824	−0.839	−0.635	0.441
	P	<0.001**	0.022*	<0.001**	0.008*	0.001*	<0.001**	<0.001**	0.434	0.008*	0.015*	0.014*	0.108
Thickness average of right isthmus cingulate	β	−2.402	−5.956	−5.322	3.569	3.251	0.375	3.607	8.392	−0.458	−0.359	−0.511	0.482
	P	<0.001**	0.005*	0.005*	<0.001**	<0.001**	0.015*	0.14	0.386	0.071	0.195	0.014*	0.027*
Subcortical volume of right amygdala	β	−0.003	−0.01	−0.01	0.003	0.004	0.001	0.009	−0.016	−0.001	−0.001	−0.001	0.001
	P	<0.001**	<0.001**	<0.001**	0.008*	<0.001**	<0.001**	<0.001**	0.109	<0.001**	0.046*	0.005*	0.017*
Subcortical volume of left amygdala	β	−0.003	−0.011	−0.01	0.004	0.004	0.001	0.009	−0.016	−0.001	0	−0.001	0
	P	<0.001**	<0.001**	<0.001**	0.001*	<0.001**	<0.001**	<0.001**	0.118	<0.001**	0.096	0.003*	0.04*
Subcortical volume of right hippocampus	β	−0.001	−0.004	−0.005	0.001	0.002	0	0.003	−0.01	−0.001	0	0	0
	P	<0.001**	<0.001**	<0.001**	0.039*	<0.001**	<0.001**	0.002*	0.03*	<0.001**	0.008*	<0.001**	0.09

Table 4 *(continued)*

Table 4 *(continued)*

Regions	Coefficience/ P value	CDRSB	ADAS 13	FAQ	MOCA	MMSE	ADNI-MEM	RAVLT-immediate	RAVLT-perc-forgetting	EcogSPVisspat	EcogSPPlan	EcogSTotal	ADNI-EF
Subcortical volume of left hippocampus	β	−0.001	−0.005	−0.004	0.001	0.002	0	0.004	−0.006	0	0	0	0
	P	<0.001**	<0.001**	<0.001**	0.021*	<0.001**	<0.001**	<0.001**	0.182	<0.001**	0.063	0.009*	0.051
Cortical volume of left entorhinal	β	−0.001	−0.004	−0.003	0.001	0.002	0	0.004	−0.002	0	0	0	0
	P	0.007*	0.005*	0.006*	0.044*	<0.001**	<0.001**	0.002*	0.692	0.07	0.573	0.272	0.919
Cortical volume of right entorhinal	β	−0.001	−0.004	−0.005	0.002	0.002	0	0.004	−0.002	0	0	0	0
	P	<0.001**	0.003*	<0.001**	0.002*	<0.001**	<0.001**	0.004*	0.697	0.005*	0.059	0.013*	0.014*
Thickness average of left entorhinal	β	−1.368	−4.072	−3.508	1.697	1.946	0.369	5.438	−4.859	−0.326	−0.229	−0.245	0.176
	P	<0.001**	<0.001**	<0.001**	0.001*	<0.001**	<0.001**	<0.001**	0.302	0.008*	0.09	0.016*	0.097
Thickness average of right entorhinal	β	−1.385	−3.543	−3.683	1.58	2.067	0.283	3.762	−3.987	−0.275	−0.191	−0.216	0.181
	P	<0.001**	<0.001**	<0.001**	0.002*	<0.001**	<0.001**	<0.001**	0.382	0.024*	0.146	0.028*	0.081

B, regression coefficient. *, P<0.05; **, P<0.001.

tests at the baseline, 12-, 24-month visits, including global cognition scales and subscales (memory, executive function, language, attention, visuospatial skills). The conclusion confirmed previous research on clinically diagnosed MCI subjects. Furthermore, the cognitive declines also supported by the frame work that the LMCI individuals degenerated faster than the EMCI ones in both global cognition function and the sub-domains. This is consistent with what had been widely believed that disease progression is slow during the earliest stages of AD (4). Landau *et al.* (26) had verified that although both hypometabolism and β-amyloid (Aβ) deposition are detectable in normal subjects and all diagnostic groups, Aβ showed greater associations with a cognitive decline in the normal participants, and has an early and subclinical impact on the cognition of individuals that precedes these metabolic changes (27). At moderate and later stages of disease (LMCI/AD), hypometabolism becomes more pronounced and more closely linked to the ongoing cognitive decline. Hence, effectively preventive treatments are urgently needed at early phases of the AD spectrum (5). In addition, we detected that LMCI participants had higher informant-report ECog scores than the EMCI participants, and both groups showed no difference in the self-reported ECog scores. Swinford (28) had found that self-and informant-ECog memory scores were not correlated with one another in the amyloid-positive adults, and suggested that the two measurements of the subjective memory complaints may be independent. Drawing on his assumptions about the results in his research, we hypothesized that the participants in prodromal AD group might be involved with the more outward signs of cognitive decline that could be noticed by an observer who knew the individual well.

An MRI provides structural information about the brain and has for many years been widely used for an early detection and a diagnosis of AD. Atrophy typically starts in the medial temporal and limbic areas, subsequently spreading to parietal association areas and finally to the frontal and primary cortices. For many years, studies have focused on the single structures in the medial temporal lobe for the early diagnosis of AD, such as hippocampus and entorhinal cortex (29). However, the MRI imaging measurement of cortical thickness, e.g., medial temporal atrophy, is still not sufficiently accurate on its own to serve as an absolute diagnostic criterion for the clinical diagnosis of AD at the MCI stage (30). There is still a lack of sensitive, reliable, and accessible brain imaging algorithms

capable of characterizing the abnormal degrees of age-related cerebral atrophy, as well as accelerated rates of atrophy progression in the preclinical individuals at a high risk for AD for whom early intervention is most needed. In this study, we use FreeSurfer image analysis suite, both longitudinal and cross-sectional processing (each scan is segmented according to an atlas defined by FreeSurfer), which produces regional volume, cortical thickness, grey matter volume, surface area, to investigate different patterns of atrophy instead of single measures, and more sensitive and predictive variable of MRI in cognitive decline.

By investigating the relationship between the structural MRI and cognitive decline, we detected that the regions significantly related to cognitive function are the bilateral hippocampus, right parahippocampal, left middle and superior temporal, bilateral amygdala, bilateral cingulate, both thickness average and cortical volume of bilateral entorhinal. Atrophy of these structures was regarded as a typical finding in AD (31). Grothe *et al.* (32) have confirmed that Episodic memory decline in the MCI patients was associated with a hippocampal atrophy and basal forebrain degeneration in the Aβ+ subjects. Attentional control was associated with a basal forebrain degeneration in the MCI subjects. Worsening impairment of the instrumental activities of daily living was associated with a baseline middle frontal and posterior cingulate hypometabolism and predicted by the baseline parietal and temporal atrophy (33). Furthermore, our findings also showed that the thickness average of the left superior temporal and bilateral entorhinal cortex mostly contributes to memory loss. Thickness average of left middle temporal and right isthmus cingulate mainly influenced executive function. The results indicated that the different MCI categories or multi-domains MCI have different clinical prognoses and biomarkers signatures, and that neuroimaging biomarkers based on the single-area ROI might not be sensitive enough for the initial stages of cognitive impairment. Further studies are needed to characterize what underlying pathologies are involved in each specific MCI group.

By now, MRI is still the most commonly used imaging examination for general clinical practice. Thus, we expect that the data from structural MRI can be one potential marker for MCI.

This study does have some potential limitations. First, although we included all available A+T+MCI participants in ADNI-2 who had PET scans and CSF p-tau at the time of our analyses, our sample size was relatively small, which could lead to bias. Second, we also acknowledge that there may have been unforeseen selection bias in the ADNI-2 study. Participants were recruited from memory clinics and advertisements, and the MCI inclusion criteria was highly selective, thus the study group is not representative of the general population. Future studies in larger samples will help to support the present findings. Finally, we used Talairach Daemon to define the brain regions from our voxel wise analysis. Although this atlas is not specific to our study, we felt that it was the most appropriate tool to use in this case. A standardized atlas specific for MCI subjects or older adults has not been defined in the literature, and our small sample size kept us from producing our own study-specific atlas. We do not expect that extensive atrophy should confound the results of the Talairach Daemon atlas in our preclinical AD population, and we visually inspected the labeled regions for accuracy. However, we acknowledge that use of this nonspecific atlas may have caused minor labeling issues in our participants.

In summary, the present study demonstrated an updated comprehensive evaluation of clinical cognition and structural MRI in the EMCI and LMCI population based on the AT (N) system. The findings will be helpful in understanding the property of prodromal AD.

Acknowledgements

Data collection and sharing for this project was funded by the Alzheimer's Disease Neuroimaging Initiative (ADNI) (National Institutes of Health Grant U01 AG024904) and DOD ADNI (Department of Defense award number W81XWH-12-2-0012). ADNI is funded by the National Institute on Aging, the National Institute of Biomedical Imaging and Bioengineering, and through generous contributions from the following: AbbVie, Alzheimer's Association; Alzheimer's Drug Discovery Foundation; Araclon Biotech; BioClinica, Inc.; Biogen; Bristol-Myers Squibb Company; CereSpir, Inc.; Cogstate; Eisai Inc.; Elan Pharmaceuticals, Inc.; Eli Lilly and Company; EuroImmun; F. Hoffmann-La Roche Ltd and its affiliated company Genentech, Inc.; Fujirebio; GE Healthcare; IXICO Ltd.; Janssen Alzheimer Immunotherapy Research & Development, LLC.; Johnson & Johnson Pharmaceutical Research & Development LLC.; Lumosity; Lundbeck; Merck & Co., Inc.; Meso Scale Diagnostics, LLC.; NeuroRx Research; Neurotrack Technologies; Novartis Pharmaceuticals Corporation; Pfizer Inc.; Piramal Imaging; Servier; Takeda Pharmaceutical Company; and Transition Therapeutics. The Canadian Institutes of Health Research

is providing funds to support ADNI clinical sites in Canada. Private sector contributions are facilitated by the Foundation for the National Institutes of Health (www.fnih.org). The grantee organization is the Northern California Institute for Research and Education, and the study is coordinated by the Alzheimer's Therapeutic Research Institute at the University of Southern California. ADNI data are disseminated by the Laboratory for Neuro Imaging at the University of Southern California.

Funding: This study was funded by the Chinese National Natural Science Foundation (No. 81571234), Key Research and Development Plan of Shandong Province (2018GSF118235), Shandong Province Medical Science and Technology Development Projects (2014WS0260) and Yantai Science and Technology Development Project (2014WS035, 2016WS037).

Footnote

Conflicts of Interest: The authors have no conflicts of interest to declare.

Ethical Statement: All procedures performed in studies involving the ADNI participants were carried out in accordance with the Helsinki declaration. The ADNI study was approved by the Institutional Review Boards of all of the participating institutions. Informed written consent was obtained from all participants and their legal representatives at each site prior to the collection of clinical, genetic, and imaging data.

References

1. Tiraboschi P, Hansen LA, Thal LJ, Corey-Bloom J. The importance of neuritic plaques and tangles to the development and evolution of AD. Neurology 2004;62:1984-9.
2. Jack CR Jr, Knopman DS, Jagust WJ, Petersen RC, Weiner MW, Aisen PS, Shaw LM, Vemuri P, Wiste HJ, Weigand SD, Lesnick TG, Pankratz VS, Donohue MC, Trojanowski JQ. Tracking pathophysiological processes in Alzheimer's disease: an updated hypothetical model of dynamic biomarkers. Lancet Neurol 2013;12:207-16.
3. Petersen RC, Smith GE, Waring SC, Ivnik RJ, Tangalos EG, Kokmen E. Mild cognitive impairment: clinical characterization and outcome. Arch Neurol 1999;56:303-8.
4. Sperling RA, Aisen PS, Beckett LA, Bennett DA, Craft S, Fagan AM, Iwatsubo T, Jack CR Jr, Kaye J, Montine TJ, Park DC, Reiman EM, Rowe CC, Siemers E, Stern Y, Yaffe K, Carrillo MC, Thies B, Morrison-Bogorad M, Wagster MV, Phelps CH. Toward defining the preclinical stages of Alzheimer's disease: recommendations from the National Institute on Aging-Alzheimer's Association workgroups on diagnostic guidelines for Alzheimer's disease. Alzheimers Dement 2011;7:280-92.
5. Jedynak BM, Lang A, Liu B, Katz E, Zhang Y, Wyman BT, Raunig D, Jedynak CP, Caffo B, Prince JL, Alzheimer's Disease Neuroimaging Initiative. A computational neurodegenerative disease progression score: method and results with the Alzheimer's disease Neuroimaging Initiative cohort. Neuroimage 2012;63:1478-86.
6. Roman G, Pascual B. Contribution of neuroimaging to the diagnosis of Alzheimer's disease and vascular dementia. Arch Med Res 2012;43:671-6.
7. Sorrell JM. Diagnostic and Statistical Manual of Mental Disorders-5: implications for older adults and their families. J Psychosoc Nurs Ment Health Serv 2013;51:19-22.
8. Delis DC, Massman PJ, Butters N, Salmon DP, Shear PK, Demadura T, Filoteo JV. Spatial cognition in Alzheimer's disease: subtypes of global-local impairment. J Clin Exp Neuropsychol 1992;14:463-77.
9. McKhann G, Drachman D, Folstein M, Katzman R, Price D, Stadlan EM. Clinical diagnosis of Alzheimer's disease: report of the NINCDS-ADRDA Work Group under the auspices of Department of Health and Human Services Task Force on Alzheimer's Disease. Neurology 1984;34:939-44.
10. Nelson PT, Head E, Schmitt FA, Davis PR, Neltner JH, Jicha GA, Abner EL, Smith CD, Van Eldik LJ, Kryscio RJ, Scheff SW. Alzheimer's disease is not "brain aging": neuropathological, genetic, and epidemiological human studies. Acta Neuropathol 2011;121:571-87.
11. Barnes LL, Leurgans S, Aggarwal NT, Shah RC, Arvanitakis Z, James BD, Buchman AS, Bennett DA, Schneider JA. Mixed pathology is more likely in black than white decedents with Alzheimer dementia. Neurology 2015;85:528-34.
12. Jack CR Jr, Bennett DA, Blennow K, Carrillo MC, Feldman HH, Frisoni GB, Hampel H, Jagust WJ, Johnson KA, Knopman DS, Petersen RC, Scheltens P, Sperling RA, Dubois B. A/T/N: An unbiased descriptive classification scheme for Alzheimer disease biomarkers. Neurology 2016;87:539-47.
13. Joshi AD, Pontecorvo MJ, Clark CM, Carpenter AP,

Jennings DL, Sadowsky CH, Adler LP, Kovnat KD, Seibyl JP, Arora A, Saha K, Burns JD, Lowrey MJ, Mintun MA, Skovronsky DM, Florbetapir FSI. Performance characteristics of amyloid PET with florbetapir F 18 in patients with alzheimer's disease and cognitively normal subjects. J Nucl Med 2012;53:378-84.
14. Shaw LM, Vanderstichele H, Knapik-Czajka M, Clark CM, Aisen PS, Petersen RC, Blennow K, Soares H, Simon A, Lewczuk P, Dean R, Siemers E, Potter W, Lee VM, Trojanowski JQ, Alzheimer's Disease Neuroimaging Initiative. Cerebrospinal fluid biomarker signature in Alzheimer's disease neuroimaging initiative subjects. Ann Neurol 2009;65:403-13.
15. Risacher SL, Saykin AJ. Neuroimaging and other biomarkers for Alzheimer's disease: the changing landscape of early detection. Annu Rev Clin Psychol 2013;9:621-48.
16. Shen D, Davatzikos C. Measuring temporal morphological changes robustly in brain MR images via 4-dimensional template warping. Neuroimage 2004;21:1508-17.
17. Davatzikos C, Genc A, Xu D, Resnick SM. Voxel-based morphometry using the RAVENS maps: methods and validation using simulated longitudinal atrophy. Neuroimage 2001;14:1361-9.
18. Bryant C, Giovanello KS, Ibrahim JG, Chang J, Shen D, Peterson BS, Zhu H, Alzheimer's Disease Neuroimaging Initiative. Mapping the genetic variation of regional brain volumes as explained by all common SNPs from the ADNI study. PLoS One 2013;8:e71723.
19. Desikan RS, Sabuncu MR, Schmansky NJ, Reuter M, Cabral HJ, Hess CP, Weiner MW, Biffi A, Anderson CD, Rosand J, Salat DH, Kemper TL, Dale AM, Sperling RA, Fischl B, Alzheimer's Disease Neuroimaging Initiative. Selective disruption of the cerebral neocortex in Alzheimer's disease. PLoS One 2010;5:e12853.
20. Montine TJ, Phelps CH, Beach TG, Bigio EH, Cairns NJ, Dickson DW, Duyckaerts C, Frosch MP, Masliah E, Mirra SS, Nelson PT, Schneider JA, Thal DR, Trojanowski JQ, Vinters HV, Hyman BT; National Institute on Aging; Alzheimer's Association. National Institute on Aging-Alzheimer's Association guidelines for the neuropathologic assessment of Alzheimer's disease: a practical approach. Acta Neuropathol 2012;123:1-11.
21. Hyman BT, Phelps CH, Beach TG, Bigio EH, Cairns NJ, Carrillo MC, Dickson DW, Duyckaerts C, Frosch MP, Masliah E, Mirra SS, Nelson PT, Schneider JA, Thal DR, Thies B, Trojanowski JQ, Vinters HV, Montine TJ. National Institute on Aging-Alzheimer's Association guidelines for the neuropathologic assessment of Alzheimer's disease. Alzheimers Dement 2012;8:1-13.
22. Barnes LL, Leurgans S, Aggarwal NT, Shah RC, Arvanitakis Z, James BD, Buchman AS, Bennett DA, Schneider JA. Mixed pathology is more likely in black than white decedents with Alzheimer dementia. Neurology 2015;85:528-34.
23. Rabinovici GD, Jagust WJ, Furst AJ, Ogar JM, Racine CA, Mormino EC, O'Neil JP, Lal RA, Dronkers NF, Miller BL, Gorno-Tempini ML. Abeta amyloid and glucose metabolism in three variants of primary progressive aphasia. Ann Neurol 2008;64:388-401.
24. Ossenkoppele R, Jansen WJ, Rabinovici GD, Knol DL, van der Flier WM, van Berckel BN, Scheltens P, Visser PJ, Amyloid PETSG, Verfaillie SC, Zwan MD, Adriaanse SM, Lammertsma AA, Barkhof F, Jagust WJ, Miller BL, Rosen HJ, Landau SM, Villemagne VL, Rowe CC, Lee DY, Na DL, Seo SW, Sarazin M, Roe CM, Sabri O, Barthel H, Koglin N, Hodges J, Leyton CE, Vandenberghe R, van Laere K, Drzezga A, Forster S, Grimmer T, Sanchez-Juan P, Carril JM, Mok V, Camus V, Klunk WE, Cohen AD, Meyer PT, Hellwig S, Newberg A, Frederiksen KS, Fleisher AS, Mintun MA, Wolk DA, Nordberg A, Rinne JO, Chetelat G, Lleo A, Blesa R, Fortea J, Madsen K, Rodrigue KM, Brooks DJ. Prevalence of amyloid PET positivity in dementia syndromes: a meta-analysis. JAMA 2015;313:1939-49.
25. Jack CR Jr, Bennett DA, Blennow K, Carrillo MC, Dunn B, Haeberlein SB, Holtzman DM, Jagust W, Jessen F, Karlawish J, Liu E, Molinuevo JL, Montine T, Phelps C, Rankin KP, Rowe CC, Scheltens P, Siemers E, Snyder HM, Sperling R, Contributors. NIA-AA Research Framework: Toward a biological definition of Alzheimer's disease. Alzheimers Dement 2018;14:535-62.
26. Landau SM, Mintun MA, Joshi AD, Koeppe RA, Petersen RC, Aisen PS, Weiner MW, Jagust WJ, Alzheimer's Disease Neuroimaging Initiative. Amyloid deposition, hypometabolism, and longitudinal cognitive decline. Ann Neurol 2012;72:578-86.
27. Lu FM, Yuan Z. PET/SPECT molecular imaging in clinical neuroscience: recent advances in the investigation of CNS diseases. Quant Imaging Med Surg 2015;5:433-47.
28 Swinford CG, Risacher SL, Charil A, Schwarz AJ, Saykin AJ. Memory concerns in the early Alzheimer's disease prodrome: Regional association with tau deposition. Alzheimers Dement (Amst) 2018;10:322-31.
29. Fox NC, Warrington EK, Freeborough PA, Hartikainen P, Kennedy AM, Stevens JM, Rossor MN. Presymptomatic hippocampal atrophy in Alzheimer's disease. A longitudinal

MRI study. Brain 1996;119:2001-7.
30. Frisoni GB, Fox NC, Jack CR Jr, Scheltens P, Thompson PM. The clinical use of structural MRI in Alzheimer disease. Nat Rev Neurol 2010;6:67-77.
31. Li X, Ba M, Ng KP, Mathotaarachchi S, Pascoal TA, Rosa-Neto P, Gauthier S. Characterizing biomarker features of cognitively normal individuals with ventriculomegaly. Alzheimers Dement (Amst) 2017;10:12-21.
32. Grothe MJ, Heinsen H, Amaro E Jr, Grinberg LT, Teipel SJ. Cognitive Correlates of Basal Forebrain Atrophy and Associated Cortical Hypometabolism in Mild Cognitive Impairment. Cereb Cortex 2016;26:2411-26.
33. Roy K, Pepin LC, Philiossaint M, Lorius N, Becker JA, Locascio JJ, Rentz DM, Sperling RA, Johnson KA, Marshall GA. Regional fluorodeoxyglucose metabolism and instrumental activities of daily living across the Alzheimer's disease spectrum. J Alzheimers Dis 2014;42:291-300.

Cite this article as: Wei H, Kong M, Zhang C, Guan L, Ba M; for Alzheimer's Disease Neuroimaging Initiative. The structural MRI markers and cognitive decline in prodromal Alzheimer's disease: a 2-year longitudinal study. Quant Imaging Med Surg 2018;8(10):1004-1019. doi: 10.21037/qims.2018.10.08

